

# Single mode and tunable GaSb-based VCSELs for wavelengths above 2 $\mu\text{m}$

Markus-Christian Amann<sup>a</sup>, Shamsul Arafin<sup>a</sup> and Kristijonas Vizbaras<sup>\*a</sup>

<sup>a</sup>Walter Schottky Institut, Technische Universität München, Am Coulombwall 3, Garching, Germany, 85748

## ABSTRACT

Results of single mode and tunable GaSb-based VCSELs, with emission wavelengths above 2  $\mu\text{m}$ , are presented. Devices are aimed at trace gas sensing applications and operate in two important spectral windows – 2.3  $\mu\text{m}$  and 2.6  $\mu\text{m}$ . The first one is suitable for CO detection and in the second one strong absorption lines of H<sub>2</sub>S and H<sub>2</sub>O lie. VCSELs emitting at 2.33  $\mu\text{m}$  operate in continuous-wave (CW) up to heatsink temperatures of 90 °C and deliver the maximum single-mode output power of 0.8 mW at 0°C with an aperture diameter of 6  $\mu\text{m}$ . With the introduction of inverted surface relief on top of the processed device, single mode operation has been extended up to 12  $\mu\text{m}$  large aperture devices. The maximum wavelength tuning range of 20 nm has been achieved. VCSELs emitting at 2.6  $\mu\text{m}$  operate in CW mode up to 55 °C, with the maximum single-mode output power of 0.4 mW, at -20 °C. They offer single transverse mode emission up to 9  $\mu\text{m}$  large apertures. The maximum wavelength tuning of 10 nm is presented. Finally, first applications to trace gas sensing are also presented for 2.3  $\mu\text{m}$  GaSb-based VCSELs.

**Keywords:** VCSEL, GaSb, gas sensing, semiconductor lasers, tunable lasers, single mode lasers

## 1. INTRODUCTION

The importance of sensing various hazardous gases has been growing recently due to security and environmental reasons. This creates an increasing demand in various gas-sensing systems. Until recently, various systems mainly based on electrochemical sensors have been used. However, they suffer from slow response times and ageing, when used in corrosive gas atmospheres. A perfect alternative here is offered by tunable-diode-laser-absorption-spectroscopy (TDLAS) [1-3]. TDLAS has an advantage of being a rapid and contactless technique for gas detection. Here, a tunable laser diode is used to scan the wavelength range of several nanometers with a frequency around 10 kHz. Typically, a sensor has a cell filled with gas, through which a light passes and a detector measures the intensity of transmission. Gases have sharp absorption lines at specific wavelengths, which act like fingerprints for the specie determination and, therefore, by tuning the laser wavelength one can scan through several absorption lines and identify the gases as well as their concentration. For such a TDLAS system, a longitudinal and transversal single-mode laser source is required. Additionally, it should be possible to tune the wavelength over few nanometers around the desired wavelength without mode-hopping. Finally, laser sources emitting in the near- and mid-infrared are preferable, as the absorption due to molecular vibrations is enhanced. Reasons mentioned above lead to an increased interest in developing single-mode tunable laser sources operating in the spectral range of 2 to 3  $\mu\text{m}$ , where several important gases, like CO, CH<sub>4</sub>, N<sub>2</sub>O, CO<sub>2</sub>, etc. can be addressed (see Fig. 1). For example, wavelength range around 2.3  $\mu\text{m}$  offers the first water absorption-free spectral window for CO detection, what is of great importance for industrial applications. Here, a compact sensor with low-power budget is preferable. Vertical-cavity surface-emitting lasers (VCSELs) are ideally suited, because they inherently emit in a single longitudinal mode, have larger electro-thermal wavelength tunability, low power consumption, small beam divergence and low-cost fabrication due to a possibility of on-wafer testing. From the material point of view, GaSb-based heterostructures are a perfectly suited for covering the 2 – 3  $\mu\text{m}$  range. Even though wavelength range up to 2.3  $\mu\text{m}$  has been covered by InP-based devices [4], it seems that it is the limit for this material system. Growth and fabrication of GaSb-based VCSELs is still immature, when compared to InP-based devices. The first electrically pumped GaSb-based VCSELs, operating in pulsed mode with an emission wavelength of 2.2  $\mu\text{m}$ , were reported by Baranov *et al.*[5] in 1998. It took 10 years until first electrically pumped VCSELs operating in continuous-wave (CW) and emitting around 2.3  $\mu\text{m}$ , were reported by Bachmann *et al.* [6].

\*Kristijonas.Vizbaras@wsi.tum.de; phone +49 289 11455; fax +49 289 12704; www.wsi.tum.de

This led to a rapid development of GaSb-based VCSEL technology and the first single-mode electrically-pumped devices with an emission wavelength around 2.6  $\mu\text{m}$  have been reported by Arafin *et al.* in 2009 [7].

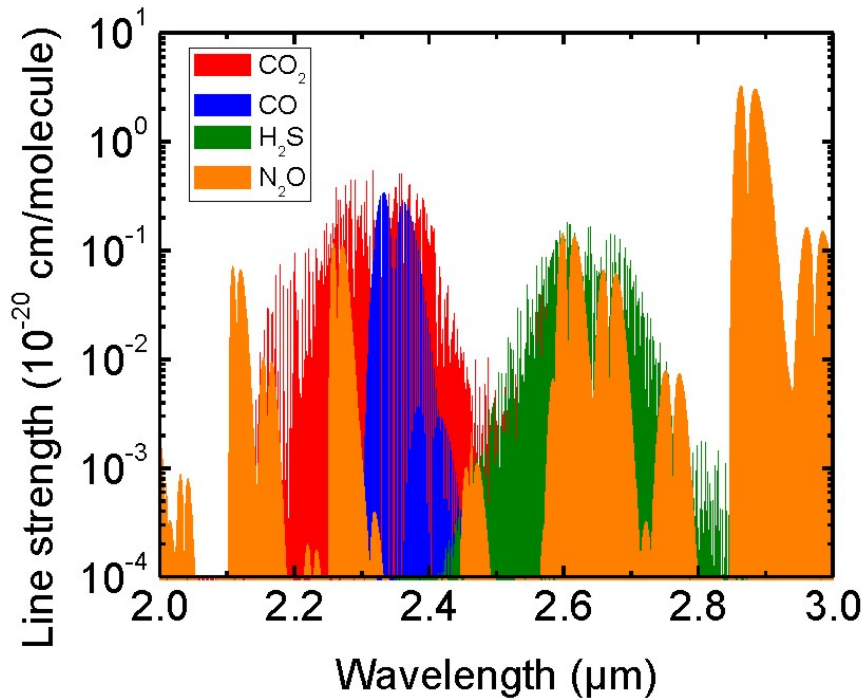


Figure 1. Absorption lines of CO, CO<sub>2</sub>, H<sub>2</sub>S and N<sub>2</sub>O as a function of wavelength, in the spectral range from 2 to 3  $\mu\text{m}$ . Data taken from [8].

In this work, we present recent progress on GaSb-based VCSELs emitting above 2  $\mu\text{m}$ . The design and device fabrication, as well as device results of such electrically-pumped index-guided buried-tunnel junction (BTJ) VCSELs emitting around 2.3  $\mu\text{m}$  and 2.6  $\mu\text{m}$  are reported here. Devices operate in single mode and are suited for CO, CH<sub>4</sub> and H<sub>2</sub>S sensing.

## 2. DEVICE FABRICATION

VCSEL structures (Fig. 2) were grown by molecular beam epitaxy (MBE) using a solid-source Varian Mod Gen-II reactor with valved cracker cells for Sb<sub>2</sub> and As<sub>2</sub>. Epitaxial growth of the device consists of two steps – in a first step a lattice matched AlAs<sub>0.08</sub>Sb<sub>0.92</sub>/GaSb distributed Bragg mirror (DBR), doped with Te to the level of  $5 \cdot 10^{17} \text{ cm}^{-3}$ , is grown. DBR is followed by *n*-doped GaSb current spreading layers and the active region, consisting of highly compressively strained (1.6%) GaInAsSb quantum wells. The first growth step is finished with a  $p^{++}$ -GaSb/ $n^{++}$ -InAsSb tunnel junction ( $p=n=2 \cdot 10^{19} \text{ cm}^{-3}$ ). After the first growth step, the devices are taken out from the MBE chamber and intracavity contacts (circular and elliptical) are defined by standard lithography and the following dry etching procedure. The samples are cleaned chemically and loaded into the chamber again. Here, an additional atomic hydrogen cleaning procedure is performed in high vacuum chamber, in order to remove remaining oxides and carbon contamination [9]. Only then the second epitaxial growth step is done, during which *n*-doped GaSb layer is grown and the structure is finalized by the growth of a low-resistive  $n^{++}$ -InAsSb contact layer.

After the MBE growth, VCSEL mesas are formed by Cl<sub>2</sub> reactive ion etching. Then, mesas are passivated by sputtering 200 nm of SiO<sub>2</sub>. This is followed by a lift-off step, where top contact is opened and wet-chemically structured

into a ring structure, thus opening a top laser facet. Then, Ti/Pt/Au metal contacts are deposited on top, which form a low-resistive ohmic metal/ $n^{++}$ -InAsSb contact [10]. On the backside, a large area Ti/Pt/Au contact is evaporated directly

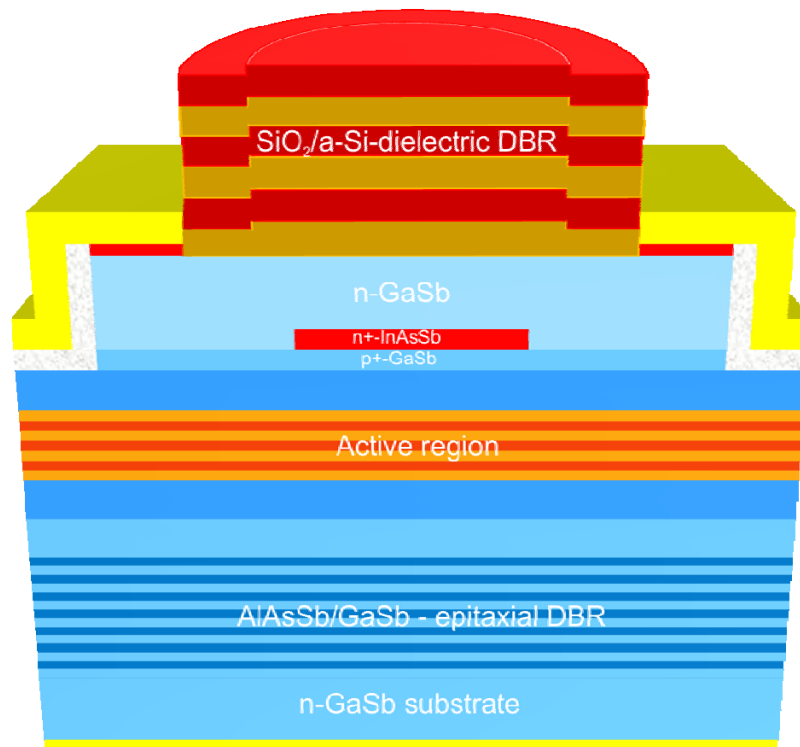


Figure 2. GaSb-based BTJ VCSEL structure. The structure is composed of an epitaxial AlAsSb/GaSb DBR, on top of which  $n$ -GaSb current spreading layers and MQW active region are grown. A BTJ above the active region serves as a current aperture. The structure is finalized with a dielectric a-Si/SiO<sub>2</sub> DBR.

on the substrate. The process is finished with the e-beam evaporation of a top dielectric DBR, consisting of 4 pairs of amorphous Si/SiO<sub>2</sub> stack.

### 3. DEVICE DESIGN

#### 3.1 Optical design

Due to a very short cavity of a VCSEL, the gain length is limited to few micrometers and, therefore, highly reflective mirrors are required. The latter is achieved by using a distributed Bragg reflector, which is composed of quarterwave thick stacks of alternating layers of high- and low-refractive index. In GaSb-based VCSELs, a bottom DBR is composed of lattice-matched AlAs<sub>0.08</sub>Sb<sub>0.92</sub> and GaSb alternating stack. Such a combination gives a refractive index difference  $\Delta n \approx 0.7$  at 2.3  $\mu\text{m}$  and has the advantage of achieving high reflectivity with relatively small number of pairs (typically around 24, for 2.3  $\mu\text{m}$  VCSEL). The maximum reflectivity, however, is limited to 99.8 % by free carrier absorption [11], because of  $n$ -doping in the epitaxial DBR layers. The top mirror is a dielectric DBR (see Fig. 2). Here a combination of a-Si/SiO<sub>2</sub> gives a refractive index difference  $\Delta n \approx 1.9$  (at 2.3  $\mu\text{m}$ ) and only four pairs are sufficient to achieve a reflectivity of 99.7 %. Optical cavity design also requires special attention, as inside it, one has a very highly doped BTJ layers and current spreading layers and additional care has to be taken in order to achieve low losses and keep the cavity short at the same. This is done by implementing  $3\lambda$ -thick cavity, where current spreader is placed in between epitaxial DBR and active region and three such spreading layers in between the BTJ and dielectric DBR in order to keep electrical resistance low. Finally, a very important thing in the optical design is to place a node of the standing wave in the tunnel junction and an anti-node in the active region.

### 3.2 Electrical design

In order to achieve a single mode operation, a current aperture is necessary for a VCSEL. Since oxide apertures with sufficient blocking up to now have not been realized yet, a BTJ is used. In our GaSb-based VCSELs, a BTJ is made from lattice matched  $n^{++}\text{-InAs}_{0.91}\text{Sb}/p^{++}\text{-GaSb}$  layers, which result in a broken gap (type-III) alignment, which is inherently favoring tunneling. Another advantage here is that for tunnel junction layers Si as a dopant can be used, due to its amphoteric character. Such a tunnel junction lead to low-resistive intracavity contacts with specific resistivities around  $2.5 \cdot 10^{-6} \Omega \cdot \text{cm}^2$  [12]. The blocking part around the structured BTJ is realized by overgrowing it with  $n\text{-GaSb}$ . In such a way, a blocking  $np^+$  junction is formed, yielding blocking ratios (current density through the tunnel junction divided by the current density through the blocking part) around 20000 [13]. Thus, the current injected through the top ring contact is effectively confined to a BTJ and the pumped area is restricted to the BTJ diameter and additional radial broadening due to carrier diffusion in the quantum wells.

## 4. DEVICE RESULTS

### 4.1 2.3 $\mu\text{m}$ VCSEL results

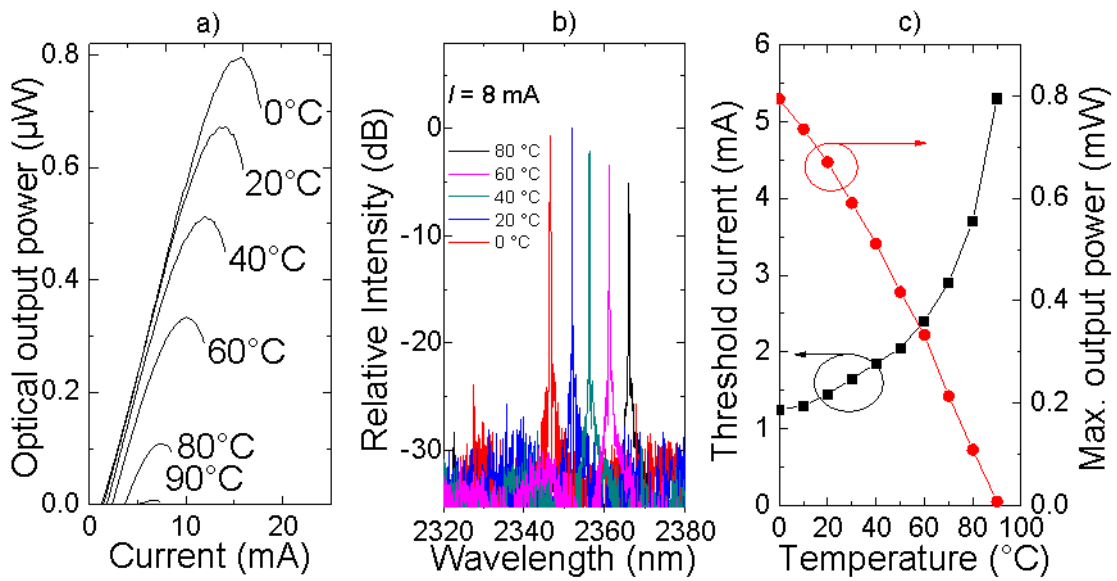


Figure 3. a)  $L$ - $I$  characteristics of a 2.3  $\mu\text{m}$  VCSEL with 6  $\mu\text{m}$  BTJ diameter, at different temperatures under CW operation; b) emission spectra of a VCSEL with 6  $\mu\text{m}$  wide BTJ at driving current of 8 mA, at different temperatures; c) Threshold current and maximum optical output power as a function heatsink temperature.

Fabricated devices were characterized on a temperature controlled copper stage and light output-current-temperature ( $L$ - $I$ - $T$ ) characteristics have been measured under CW operation (Fig. 3a). Devices exhibit single-mode operation, up to 90  $^{\circ}\text{C}$  heatsink temperature with an aperture diameter up to 6  $\mu\text{m}$  in diameter (Fig. 3b). The side-mode suppression ratio (SMSR) is 25 dB. At 0  $^{\circ}\text{C}$ , the maximum output power of 800  $\mu\text{W}$  is found, with a threshold current as low as 1.2 mA, corresponding to an effective threshold current density of 1.8  $\text{kA}/\text{cm}^2$ , where a radial carrier diffusion length of 1.6  $\mu\text{m}$  on each side has been considered. It can be noticed that threshold current is increasing and the optical output power is dropping with increasing temperature (Fig. 1c) and the minimum of the threshold current is below 0  $^{\circ}\text{C}$ . Such a behavior is due to an unintentionally misaligned cavity mode and gain maximum. Which is often the case in GaSb-based VCSELs, because the in-situ annealing during the overgrowth step causes a blueshift in the emission wavelength [14-16], which is difficult to predict accurately. Electro-thermal wavelength tunability of the devices has also been investigated. Wavelength shift of 1.03 nm/mA and a tuning range of 10 nm have been achieved by self-induced heating, at 20  $^{\circ}\text{C}$ . Tunability by temperature yielded a value of 0.24 nm/K and the total tuning range of 20 nm between 0 and 80  $^{\circ}\text{C}$  has been achieved. The achieved single mode output powers around 0.8 mW are already sufficient for gas sensing

and first such measurements with our devices have been carried out by Siemens, resulting in a 57 ppm detection of CO [17]. However, output powers above 1 mW would be more desirable to increase the sensitivity further. Typically, larger apertures are used to generate more output, on the other hand they emit in multiple lateral modes and are not useful for TDLAS applications. An approach, called inverted surface-relief, was used to extend the single-mode operation to larger diameter BTJ-VCSELs [18]. Here, an additional  $\lambda/4$  a-Si ring, with an inner diameter of 60% of the BTJ-diameter is deposited on top of the dielectric DBR and, in such a manner, reflectivity is reduced and losses are increased at the outer part of out-coupling mirror. Since higher-order lateral modes typically have the highest intensity away from the mesa center, their gain is reduced and fundamental lateral mode is favored. Using this technique we are able to achieve single-mode operation for BTJ diameters up to 12  $\mu\text{m}$ , however the maximum output power was limited to only 0.6 mW at 20  $^{\circ}\text{C}$ , whereas the device without ISR had an output power of 0.55 mW [19]. This is due to increasing injection inhomogeneity for larger BTJ diameters and spatial hole burning.

#### 4.2 2.6 $\mu\text{m}$ VCSEL results

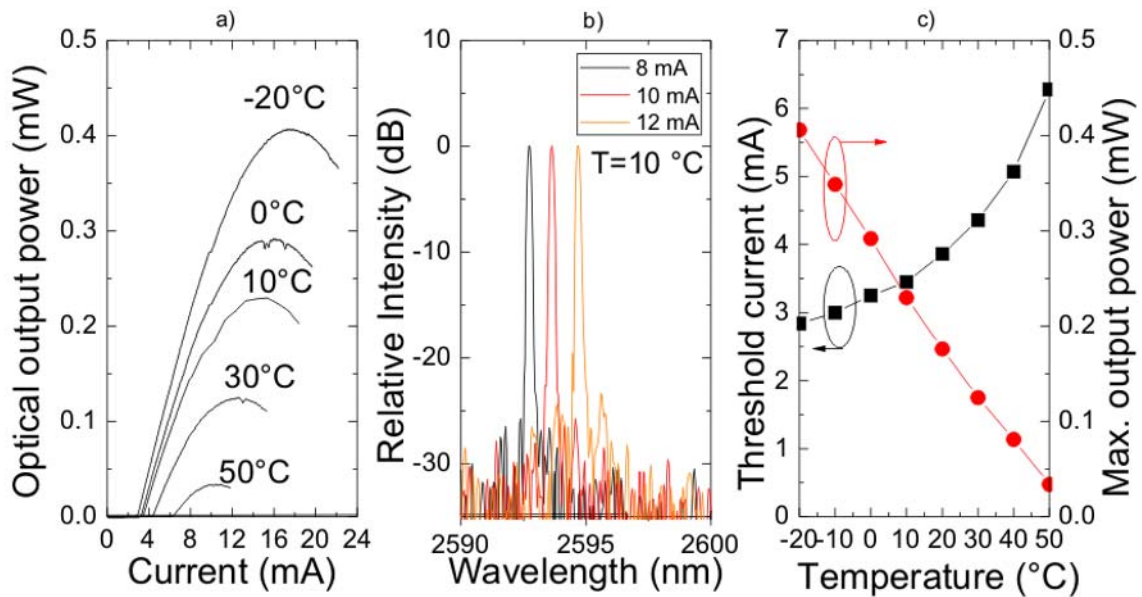


Figure 4. a)  $L$ - $I$  characteristics of a 2.6  $\mu\text{m}$  VCSEL with 6  $\mu\text{m}$  BTJ diameter, at different temperatures under CW operation; b) emission spectra of a VCSEL with 6 $\mu\text{m}$  wide BTJ at 10  $^{\circ}\text{C}$ , at different driving currents; c) Threshold current and maximum optical output power as a function heatsink temperature.

2.6  $\mu\text{m}$  VCSELs were fabricated in the same way as the ones emitting at 2.3  $\mu\text{m}$  and  $L$ - $I$ - $T$  characteristics have been measured under CW operation (Fig. 4a). Devices exhibit single-mode CW operation for mesa apertures up to 9  $\mu\text{m}$  in diameter and exhibit CW operation up to 55 $^{\circ}\text{C}$  heatsink temperature (Fig. 4a). Here, the side mode suppression ratio above 25 dB is found and a maximum output power of around 400  $\mu\text{W}$  at -20  $^{\circ}\text{C}$  has been achieved (Fig. 4b). 2.6  $\mu\text{m}$  VCSELs exhibit higher threshold current than 2.3  $\mu\text{m}$  devices, what can be expected due to increasing Auger and free-carrier losses at longer wavelengths. However, here, again, the cavity mode is misaligned with the gain, as can be seen from Fig.4c. The reasons for such a behavior are the same as explained in the previous section. The minimum threshold current lies below -20  $^{\circ}\text{C}$  and there is definitely a lot of room for performance improvement. 2.6  $\mu\text{m}$  VCSELs exhibit electro-thermal tunability of 0.5 nm/mA and an overall tuning range of 4 nm. The overall thermal tuning range of 10 nm has been achieved in the temperature range of -15 to 25 $^{\circ}\text{C}$ . A smaller current tunability than that of 2.3  $\mu\text{m}$  VCSELs can be explained by the fact that thicker current spreading layers were used, which also act as heat spreaders, and the same

change in current results in smaller change of device temperature. The extended single mode operation up to 9  $\mu\text{m}$  is due to a reduced index guiding defined by the BTJ [20].

## 5. CONCLUSIONS

In summary, single-mode and tunable VCSELs emitting around 2.3 and 2.6  $\mu\text{m}$  have been presented. Devices emitting at 2.3  $\mu\text{m}$  exhibit CW single-mode operation up to 90 °C heatsink temperature with SMSR above 20 dB. Total tuning range of 20 nm in the temperature range of 0 – 80 °C has been demonstrated. Pilot CO sensing measurements have been carried out and a sensitivity of 57 ppm has been achieved. VCSELs emitting at 2.6  $\mu\text{m}$  demonstrate CW single-mode operation up to 55 °C with a SMSR of around 20 dB. Total tuning range of 10 nm has been achieved in the temperature range from -15 to 25 °C. Such device performance shows a great potential of GaSb-based VCSELs for trace gas sensing applications.

## REFERENCES

- [1] A. Vicet, D. A. Yarekha, A. Perona, Y. Rouillard, S. Gaillard, and A. N. Baranov, "Trace gas detection with antimonide-based quantum-well diode lasers," *Spectrochim. Acta, A*, vol. 58, pp. 2405-2412, 2002.
- [2] P. Werle, "A review of recent advances in semiconductor laser based gas monitors," *Spectrochim. Acta, A*, vol. 54, pp. 197-236, 1998.
- [3] P. Werle, F. Slemr, K. Maurer, R. Kormann, R. Mücke, and B. Jänker, "Near- and mid-infrared laser-optical sensors for gas analysis," *Opt. Lasers Eng.*, vol. 37, pp. 101-114, 2002.
- [4] M. Ortsiefer, G. Böhm, M. Grau, K. Windhorn, E. Rönneberg, J. Rosskopf, R. Shau, O. Dier, and M.-C. Amann, "Electrically pumped room temperature CW VCSELs with 2.3  $\mu\text{m}$  emission wavelength," *Electron. Lett.*, vol. 42, No. 11, pp. 640-641, 2006.
- [5] A. N. Baranov, Y. Rouillard, G. Boissier, P. Grech, S. Gaillard, and C. Alibert, "Sb-based monolithic VCSEL operating near 2.2  $\mu\text{m}$  at room temperature," *Electron. Lett.*, vol. 34, No. 3, pp. 281-282, 1998.
- [6] A. Bachmann, T. Lim, K. Kashani-Shirazi, O. Dier, C. Lauer, and M.-C. Amann, "Continuous-wave operation of electrically pumped GaSb-based vertical cavity surface emitting laser at 2.3  $\mu\text{m}$ ," *Electron. Lett.*, vol. 44, No. 3, pp. 202-203, 2008.
- [7] S. Arafin, A. Bachmann, K. Kashani-Shirazi, and M.-C. Amann, "Electrically pumped continuous-wave vertical-cavity surface-emitting lasers at  $\sim$  2.6  $\mu\text{m}$ ," *Appl. Phys. Lett.*, vol. 95, No. 13, 131120, 2009.
- [8] L. Rothman et al., 'The HITRAN 2004 molecular spectroscopic database', *J. Quant.Spectrosc. Radiat. Transf.*, vol. 96, pp. 139 – 205, 2005.
- [9] G. R. Bell, N. S. Kaijaks, R. J. Dixon, and C. F. McConville, "Atomic hydrogen cleaning of polar III-V semiconductor surfaces," *Surf. Sci.*, vol. 401, pp. 125-137, 1998.
- [10] C. Lauer, O. Dier, and M.-C. Amann, "Low-resistive metal/n<sup>+</sup>-InAsSb/n-GaSb contacts," *Semicond. Sci. Technol.*, vol. 21, pp. 1274-1277, 2006.
- [11] R. A. Soref, and J. P. Lorenzo, "All-silicon active and passive guided-wave components for 1.3 and 1.6  $\mu\text{m}$ ," *IEEE J. Quantum Electron.*, vol. QE-22, No. 6, pp. 873-879, 1986.
- [12] O. Dier, C. Lauer, and M.-C. Amann, "n-InAsSb/p-GaSb tunnel junctions with extremely low resistivity," *Electron. Lett.*, vol. 42, No. 7, pp. 419-420, 2006.
- [13] A. Bachmann, K. Kashani-Shirazi, S. Arafin, and M.-C. Amann, "GaSb-based VCSEL with buried tunnel junction for emission around 2.3  $\mu\text{m}$ ," *IEEE J. Sel. Topics Quantum Electron.*, vol. 15, No. 3, pp. 933-940, 2009.
- [14] Y. Wang, H. S. Djie, B. S. Ooi, "Interdiffusion in GaInAsSb/AlGaAsSb quantum wells," *J. Appl. Phys.*, vol. 98, 073508, 2005.
- [15] Y. Wang, H. S. Djie, B. S. Ooi, P. Rotella, P. Dowd, V. Aimez, Y. Cao, Y. H. Zhang, "Interdiffusion effect on quantum-well structures grown on GaSb substrate," *Thin Sol. Films*, vol. 515, pp. 4352-4355, 2007.
- [16] O. Dier, S. Dachs, M. Grau, C. Lin, C. Lauer, M.-C. Amann, "Effects of thermal annealing on the bandgap of GaInAsSb," *Appl. Phys. Lett.*, vol. 86, No. 15, 151120, 2005.

- [17] J. Chen, A. Hangauer, A. Bachmann, T. Lim, K. Kashani-Shirazi, R. Strzoda and M.-C. Amann, "CO and CH<sub>4</sub> sensing with single-mode 2.3 μm GaSb-based VCSEL," CLEO/QELS Conference on Lasers and Electro Optics, Baltimore, USA, 2009.
- [18] E. Soderberg, J. S. Gustavsson, P. Modh, A. Larsson, Z. Z. Zhang, J. Berggren, and M. Hammar, "Suppression of higher order transverse and oxide modes in 1.3 μm InGaAs VCSELs by an inverted surface relief," IEEE Photon. Technol. Lett., vol. 9, No. 5-8, pp. 327-329, 2007.
- [19] S. Arafin, A. Bachmann, K. Vizbaras, J. S. Gustavsson, A. Larsson and M.-C. Amann, "Large-area single-mode GaSb-based BTJ VCSELs using an inverted surface relief," 23<sup>rd</sup> Annual meeting of the IEEE society (LEOS), Denver, USA, 2010.
- [20] S. Arafin, A. Bachmann, K. Vizbaras, and M.-C. Amann, "Large-aperture single-mode GaSb-based BTJ VCSELs at 2.62 μm," 22<sup>nd</sup> ISLC International semiconductor laser conference, Kyoto, Japan, 2010.